Determination of the orientation of the axial ligands and of the magnetic properties of the haems in the tetrahaem ferricytochrome from *Shewanella frigidimarina*

Ricardo O. Louro[a], Miguel Pessanha[a], Graeme A. Reid[b], Stephen K. Chapman[c], David L. Turner[a,d], Carlos A. Salgueiro[a,e,*]

[a]*Instituto de Tecnologia Química e Biológica, Universidade Nova de Lisboa, Rua da Quinta Grande 6, 2780-156 Oeiras, Portugal*
[b]*Institute of Cell and Molecular Biology, University of Edinburgh, Mayfield Road, Edinburgh EH9 3JR, UK*
[c]*Department of Chemistry, University of Edinburgh, West Mains Road, Edinburgh EH9 3JJ, UK*
[d]*Department of Chemistry, University of Southampton, Southampton SO17 1BJ, UK*
[e]*Departamento de Química da Faculdade de Ciências e Tecnologia da Universidade Nova de Lisboa, Quinta da Torre, 2825-114 Caparica, Portugal*

Abstract The unambiguous assignment of the nuclear magnetic resonance (NMR) signals of the α-substituents of the haems in the tetrahaem cytochrome isolated from *Shewanella frigidimarina* NCIMB400, was made using a combination of homonuclear and heteronuclear experiments. The paramagnetic ^{13}C shifts of the nuclei directly bound to the porphyrin of each haem group were analysed in the framework of a model for the haem electronic structure. The analysis yields g-tensors for each haem, which allowed the assignment of some electron paramagnetic resonance (EPR) signals to specific haems, and the orientation of the magnetic axes relative to each haem to be established. The orientation of the axial ligands of the haems was determined semi-empirically from the NMR data, and the structural results were compared with those of the homologous tetrahaem cytochrome from *Shewanella oneidensis* MR-1 showing significant similarities between the two proteins.
© 2002 Published by Elsevier Science B.V. on behalf of the Federation of European Biochemical Societies.

Key words: Heteronuclear nuclear magnetic resonance; Haem electronic structure; Paramagnetic shift; Electron transfer; *Shewanella*

1. Introduction

The study of haem proteins is of great interest for biological sciences due to their metabolic importance in a wide range of biological tasks, such as electron transfer [1], small molecule binding and transport [2], catalysis and energy conservation [3], and cell signalling [4].

The tetrahaem cytochrome isolated from *Shewanella frigidimarina* NCIMB400 (*Sfc*) is one among several periplasmic *c*-type cytochromes that is produced by the bacterium under anaerobiosis [5]. This cytochrome was shown to be involved in

the respiration of Fe(III) [6], one of the several terminal respiratory electron acceptors that this organism can utilise [7,8]. Sequence analysis and electron paramagnetic resonance (EPR) studies suggested that all the haem groups in *Sfc* are axially coordinated by two histidine residues [6], and this was confirmed by a preliminary determination of the reduced *Sfc* haem core architecture in solution by nuclear magnetic resonance (NMR) techniques [9]. This structural study revealed that the haem core architecture of *Sfc* is similar to that of the N-terminal domain of the soluble fumarate reductase flavocytochrome c_3 [10], also produced by *S. frigidimarina* under anaerobic growth conditions [11,12]. The recently determined crystal structure of a similar cytochrome from *Shewanella oneidensis* MR-1 is in agreement with these findings [13].

NMR is an important tool for structural and functional studies of haem proteins, and the electronic structure of low spin paramagnetic haems can be determined on the basis of ^{13}C NMR data. This provides information on the orientation of the haem axial ligands and the magnetic properties of the unpaired electron [14–17]. Empirical equations have also been presented that allow the geometry of the axial ligands to be determined using the observed ^{1}H chemical shift of the haem methyls at 298 K [18,19]. Since the orientation of the magnetic axes can be deduced from the orientation of the axial ligands [20], both approaches allow the information contained in paramagnetic shifts to be used for solution structure refinement [21–24].

In this work, the electronic structure of the four haems in the *Sfc* was determined and used to establish the orientation of the planes of the axial histidines, and the orientation of the magnetic axes relative to each haem. The g-tensors for each haem were calculated, which allowed the assignment of the some EPR signals to the structure.

2. Materials and methods

The *Sfc* was purified as described previously [6]. The protein was lyophilised twice with ^{2}H$_2$O (99.96% atom), dissolved in the same solvent to a final concentration of approximately 3 mM, and the pH adjusted to 6.1 by addition of 0.1 M NaO^{2}H or ^{2}HCl without correction for the isotope effect.

NMR experiments were performed on a Bruker DRX500 spectrometer equipped with a 5 mm inverse detection probe head with internal

*Corresponding author. Fax: (351)-21-4428766.
E-mail address:* cas@itqb.unl.pt (C.A. Salgueiro).

Abbreviations: Sfc, Shewanella frigidimarina NCIMB400 tetrahaem cytochrome; NOESY, nuclear Overhauser spectroscopy; TOCSY, total correlation spectroscopy; HMQC, heteronuclear multiple quantum coherence; *Soc, Shewanella oneidensis* MR-1 tetrahaem cytochrome
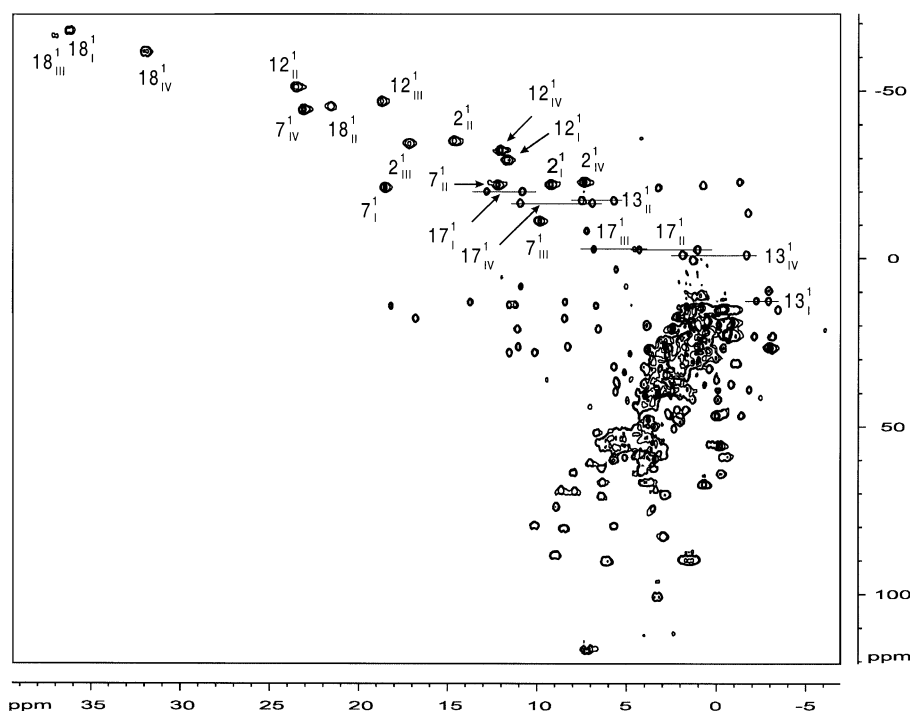
Fig. 1. ^{1}H–^{13}C HMQC spectrum of *Sfc* obtained at 35.7°C. Labels indicate the haem substituents according to IUPAC-IUB nomenclature with roman numbers for the four haems in the order of their binding sites in the protein sequence.

B_0 gradient coils and a Eurotherm 818 temperature control unit at 25.1°C and 35.7°C. Nuclear Overhauser spectroscopy (NOESY) spectra were collected with a mixing time of 35 ms and a sweep width of 40 kHz in both dimensions. Total correlation spectroscopy (TOCSY) experiments were performed with 30 ms mixing time and a sweep width of 14.7 kHz. The ^{1}H–^{13}C heteronuclear multiple quantum coherence (HMQC) spectra obtained from natural abundance samples were acquired with a sweep width of 40 kHz in F_2 and 30.7 kHz in F_1.

One-dimensional (1-D) ^{1}H NMR spectra were measured at various temperatures to follow the temperature dependence of the paramagnetically shifted haem methyl signals.

^{1}H chemical shifts were calibrated using the water signal as internal reference [25], and the ^{13}C chemical shifts calibrated using the [3-^{13}C] signal of lactate at 20.6 ppm.

3. Results

3.1. Resonance assignment

The 16 haem methyl proton signals were assigned in the diamagnetic ferrocytochrome using two-dimensional NMR

Table 1
Structural assignment of the ^{1}H and ^{13}C resonances to the substituents of the four haems of *Sfc* at 25.1 and 35.7°C, pH = 6.1

T (°C)	Group	Haem I		Haem II		Haem III		Haem IV	
		^{13}C	^{1}H	^{13}C	^{1}H	^{13}C	^{1}H	^{13}C	^{1}H
35.7									
	2^1	−22.4	9.25	−35.4	14.66	−34.6	17.19	−23.1	7.37
	3^1		0.43*		1.34*			15.24*	−3.43*
	7^1	−21.6	18.54	−22.3	12.21	−11.4	9.88	−44.8	23.11
	8^1			−13.81*	−1.77*				
	12^1	−29.7	11.70	−51.4	23.57	−47.1	18.72	−32.7	12.07
	13^1	12.6	−2.21	−17.6	7.51	26.5*	−0.40*	−1.2	1.93
			−2.88		5.74		−2.95*		−1.66
	17^1	−20.3	12.84	−2.8	4.33	−3.0	6.85	−16.9	10.96
			10.84		1.08		4.60		6.93
	18^1	−68.0	36.29	−45.7	21.6	−66.5	37.09	−61.9	32.00
25.1									
	2^1	−24.0	9.50	−37.7	15.10	−36.3	17.75	−24.3	7.10
	3^1		−0.91*		1.09			15.39*	−3.94*
	7^1	−22.6	18.90	−23.0	11.96	−12.2	10.00	−47.6	23.85
	8^1			−15.98*	−2.27*				
	12^1	−31.7	12.10	−54.5	24.40	−49.6	19.30	−34.3	11.89
	13^1	12.7	−2.49	−18.94	7.41	26.0	−0.57	−1.6	1.42
			−3.48		5.55		−3.37		−2.35
	17^1	−21.8	12.93	−3.4	4.09	−3.7	6.86	−18.6	11.00
			10.81		0.57		4.40		6.90
	18^1	−71.8	37.50	−47.9	22.24	−69.5	38.40	−65.4	33.20

The symbol * denotes tentative assignments.

spectroscopy techniques [9]. All but three haem methyl groups were cross-assigned to their positions in the spectrum of the fully oxidised protein using two-dimensional NMR exchange experiments [9]. The three haem methyls that can not be followed are $2^1CH_3^{III}$, $7^1CH_3^{III}$, and $12^1CH_3^{III}$ (roman numbers refer to the haem order attachment to the polypeptide chain). These haem methyl groups have small paramagnetic chemical shifts at lower fractions of protein oxidation and appear in a very crowded region of the NMR spectra. In fact, haem III was shown to be the last haem to oxidise, which explains the small chemical shift of its methyls in the early stages of oxidation [9].

The ^{13}C resonances of the nuclei directly attached to the porphyrin rings, and respective protons, were specifically assigned by combining the data from NOESY, TOCSY and ^1H–^{13}C HMQC (Fig. 1) experiments obtained for the oxidised protein, following the strategy described for *Desulfovibrio vulgaris* cytochrome c_3 [15,26]. This strategy was successfully applied to *Sfc* and confirmed independently the specific assignment of the haem methyl groups followed by 2-D NMR exchange experiments. The ^1H and ^{13}C chemical shifts measured for the carbons directly bonded to the porphyrin ring and respective protons in the *Sfc* oxidised cytochrome are listed in Table 1 (IUPAC-IUB nomenclature is used throughout the paper for the haem substituents). The data reported as tentative were not used in the calculations of the haem electronic structure.

3.2. Determination of the haem electronic structure

The model for analysing the ^{13}C shifts of haem signals in terms of the haem molecular orbitals can only be applied when there is no contribution of high-spin states to the ob-
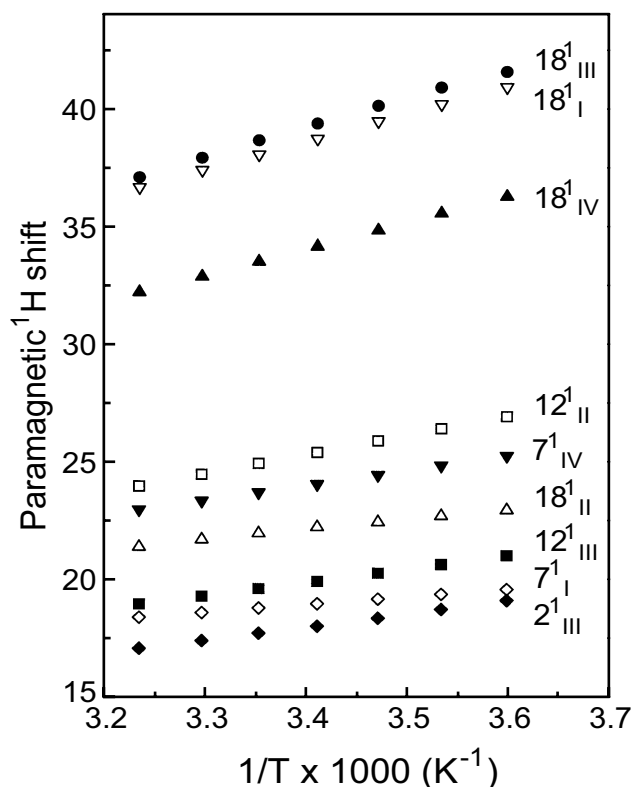

Fig. 2. Temperature dependence of the downfield shifted haem methyl signals of *Sfc*. Labels as in Fig. 1.
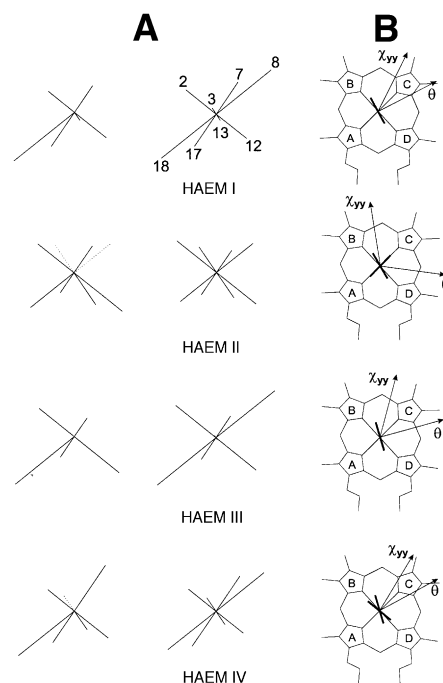

Fig. 3. Experimental and calculated ^{13}C shifts of haem substituents and orientation of the axial ligands derived from these data. A: Paramagnetic ^{13}C shifts of the α-substituents of the porphyrin. The values were calculated from the experimental data reported in Table 1 corrected for the diamagnetic references (12.1 ppm for methyls, 36.5 ppm for thioethers and 22.5 ppm for α-propionates) reported in the literature [27]. For each of the four haems, the left column represents the experimental shift by the length of the lines directed towards the pyrrole carbons that bear the substituent, with the iron at the origin. The right column shows the calculated contact shifts from the fitting reported in Table 2. For clarity, the lines for haem I were labelled according to IUPAC-IUB nomenclature for the pyrrole carbon that bears the substituent. B: Orientation of the axial histidine planes projected onto the haem determined from the fitting of the ^{13}C NMR data to the model of haem molecular orbitals. The histidine planes of haems I and III are occluded. The orientations of the rhombic perturbation and of the magnetic χ_{yy} axis are also shown. The haem pyrrole rings are labelled according to the nomenclature of Fisher.

served chemical shifts [15]. Fig. 2 shows the temperature dependence of the ^1H signals arising from the haem methyls. All signals, including those at lowest field, display a linear dependence of the chemical shift with temperature, which indicates that there are no contributions from high-spin states in the temperature range 5–35.7°C.

Fig. 3A represents schematically the experimental and calculated paramagnetic ^{13}C shifts of the carbons directly bonded to the porphyrin ring and shows that the pattern of shifts is well described by the model for the haem molecular orbitals [15]. The results of the fit of the model to the ^{13}C data at the two temperatures are reported in Table 2.

The parameter θ represents the orientation of the rhombic perturbation that mixes the frontier molecular orbitals of the haem. It is defined relative to the N_C–N_A axis of the porphyrin with positive angles between N_C, N_B and N_A [27]. The orientation of the rhombic perturbation has been found to agree with the orientation of the bisector of the angle defined by the normals to the planes of the axial ligands [19]. Also, in several bis-histidine cytochromes for which the principal axes of the magnetic susceptibility tensor have been determined

Table 2
Parameters obtained by fitting the model of haem molecular orbitals to the ^{13}C shifts of the haem substituents, and geometric parameters of the axial ligands derived from those parameters

Parameter	Haem I	Haem II	Haem III	Haem IV
θ (°)	−17.6 (0.3)	−53 (1)	−29.5 (0.4)	−13.3 (0.3)
ΔE (kJ/mol)	6.5 (0.2)	1.66 (0.04)	5.6 (0.2)	4.0 (0.1)
β (°)	0	73	0	34

The values in parentheses indicate the standard error associated with the molecular orbital parameters assuming that the chemical shifts have an experimental uncertainty of 1 ppm. The hyperfine coupling constant (Q_{CC}) was set to the value of −36 MHz, previously determined from a large collection of multihaem cytochromes c [16].

independently, θ agrees very well with the negative in-plane rotation of the axis χ_{yy}.

It has been shown that the energy splitting of the frontier molecular orbitals (ΔE) has a similar value to the rhombic splitting of the Kramers doublets that arise from mixing d_{xz} and d_{yz} orbitals of the iron when it is in a cubic crystal field with axial and rhombic distortions [27]. Hence, the g-tensor associated with each haem can be calculated from the data reported in Table 2 by assuming the value of 2.83λ for the axial splitting, obtained by fitting data from several bis-histidine haems, with λ equal to 279 cm^{-1} [17].

Finally, ΔE has been found to relate to the acute angle β between the axial ligand planes via the empirical equation $\Delta E = (5+\cos 4\theta)\cos \beta$ [16].

4. Discussion

Fig. 1 shows the assignment of the great majority of the paramagnetically shifted resonances in the ^1H–^{13}C HMQC spectrum. As reported in Table 1, only a few haem signals are either unassigned or remain tentative, and these are located in spectral regions which are crowded either in the proton or carbon frequency or both.

The results reported in Table 2 show that haems I and III are very similar with respect to the orientation of the haem axial ligands. Indeed, as shown in Fig. 3, the axial histidines are expected to have parallel planes that lie within the sector defined by the vectors N_A–Fe and Fe–N_D. Haems with parallel histidine ligands have rhombic EPR signals [28] and, given the approximations in the calculation [27,29], the results are in good agreement with the principal values $g_z = 2.83$, $g_y = 2.22$ and $g_x = 1.53$ observed in the EPR spectrum [6] (Fig. 4). The
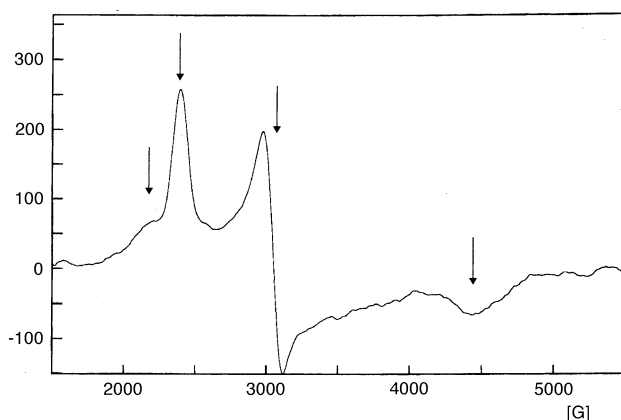
g-values calculated for haems I and III are reported in Table 3 and it is evident that the EPR signals arising from these two haems must be strongly overlapped. It should be noted that the energy splitting of the orbitals obtained for haem I is slightly larger than the expected maximum of 6 kJ/mol for bis-histidine coordination of a low spin haem [16]. The energy splitting is determined from the anisotropy of the shifts of the haem substituents, which the model assumes will have inversion symmetry with respect to the iron, and from the temperature dependence of those shifts. Fitting the data at each temperature did not alter the resulting splitting, which indicates that the pattern of shifts is indeed more anisotropic than expected. It is common to observe some asymmetry between the shifts of diametrically opposed substituents, which may be caused by the presence of other paramagnetic haems or distortions of the haem macrocycle [16]. The analysis of ^{13}C shifts normally has the advantage of averaging pairs of substituents but, in this case, the 8^1CH resonance was not found. The ^1H shifts of 18^1CH_3 are also unusually large in haems I and III, exceeding the maximum values predicted by the empirical formulae [18,19] by about 2 ppm.

The NMR data indicate that haem IV has a value of θ similar to that observed for haem I, with a smaller value of ΔE from which we predict a dihedral angle of 34° between the axial ligand planes and a value of 3.21 for g_z. The broad shoulder observed in the EPR spectrum at $g > 3$ certainly includes a contribution from this haem. Furthermore, the value of g_y at 2.10 may be responsible for the asymmetry of the strong signal at $g = 2.20$.

Haem II has a very small value of ΔE, which makes this haem the most nearly axial of the four and predicts a large dihedral angle β between the axial ligand planes (see Fig. 3B). The calculated g-values are $g_z = 3.61$, $g_y = 1.48$ and $g_x = 0.28$. The values of g_x and g_y are too low to be easily observable in the EPR spectrum, and the g_z signal, which may be broadened by slight heterogeneity of the ligand orientations in the frozen sample, may be associated with the broad shoulder that also includes the g_z-value of haem IV. The orientation of the rhombic perturbation becomes less well defined as the haem approaches axial symmetry, which is reflected in the larger standard error associated with the parameter θ for haem II

Fig. 4. X-band EPR spectrum of *Sfc* measured at pH 7.0 at 10 K [6]. Arrows indicate the spectral features discussed in the text.

Table 3
g-Values calculated for the four haems using the energy of rhombic splitting obtained from the model for the haem molecular orbitals with an axial splitting of 2.83λ, with $\lambda = 279$ cm^{-1} [17]

g-value	Haem I	Haem II	Haem III	Haem IV
g_z	2.89	3.61	2.99	3.21
g_y	2.31	1.48	2.26	2.10
g_x	1.49	0.28	1.38	1.10

and, hence, for the orientation of the ligands. In the limit, the rhombic perturbation vanishes and its orientation is totally undetermined, but the conclusion that the ligand planes have near-perpendicular relative orientations remains valid.

The geometry of the axial ligands of cytochromes may also be determined from the paramagnetic ^{1}H shifts of the haem methyls at 298 K using the empirical methods described in the literature [18,19]. However, given the close spatial proximity of haems II and III in this multihaem cytochrome, particularly for pyrrole rings A and B [9], and the greater sensitivity of ^{1}H to extrinsic pseudo-contact shifts generated by neighbouring haems, those methods are not expected to give reliable results.

Recently, a structure of the soluble periplasmic tetrahaem cytochrome from *S. oneidensis* MR-1 (*Soc*) was published [13]. In that work, the authors state that haems I and III have parallel axial ligands and haems II and IV have perpendicular axial ligands. This statement is in qualitative agreement with the EPR spectrum for that protein [30], which is similar to the EPR spectrum of *Sfc* with a clear set of rhombic and axial signals. Thus, the structural information obtained in this work and from the X-ray structure of *Soc*, together with the spectroscopic information obtained by EPR for the two proteins shows that the two proteins are very similar with respect to the orientation of the axial histidines of the haems, as well as the relative orientations of the haems themselves. This is not always the case as was observed for the cytochromes c_3 from the *Desulfovibrionaceae* family in which there is considerable scatter in the orientation of the axial histidines in structurally homologous proteins [16].

5. Conclusions

This study allowed the electronic structure of the paramagnetic haems of *Sfc* to be determined, which defines the orientation of the axial ligands relative to the haem plane [15]. The results show that the *Sfc* and *Soc* are very similar with respect the geometry of the haem ligands. These data are also important for refining solution structures of the ferricytochrome given the difficulty in measuring NOE volumes in the vicinity of the paramagnetic haem. First, the orientations of the axial histidines may be constrained within the range of experimental error. Since the analysis considers only the ligand plane, the results are eight-fold degenerate with respect to the actual orientation of the δ_2 and ε_1 carbons of the axial histidines. However, the degeneracy may be lifted by reference to preliminary calculated structures [24,31]. Furthermore, this analysis provides constraints on the orientation of the magnetic susceptibility tensor of each haem, which determines the pseudo-contact shifts experienced by nuclei throughout the protein. The *z* axis is typically found within a few degrees of the normal to the haem plane, and the *y* axis is rotated through the negative of the angle θ. Constraining the orientation of the magnetic axes improves both convergence and resolution when pseudo-contact shifts, which provide important additional geometric constraints, are included in the calculation of solution structures of molecules with paramagnetic centres [23].

References

[1] Pereira, I.A.C., Teixeira, M. and Xavier, A.V. (1998) in: Structure and Bonding Vol. 91, pp. 65–89, Springer, Berlin.

[2] Eaton, W.A., Henry, E.R., Hofrichter, J. and Mozzarelli, A. (1999) Nat. Struct. Biol. 6, 351–358.

[3] Wikstrom, M. (1998) Curr. Opin. Struct. Biol. 8, 480–488.

[4] Groves, J.T. (1999) Curr. Opin. Chem. Biol. 3, 226–235.

[5] Myers, C.R. and Myers, J.M. (1992) J. Bacteriol. 174, 3429–3438.

[6] Gordon, E.H.J., Pike, A.D., Hill, A.E., Cuthbertson, P.M., Chapman, S.K. and Reid, G.A. (2000) Biochem. J. 349, 153–158.

[7] Myers, C.R. and Nealson, K.H. (1988) Science 240, 1319–1321.

[8] Myers, C.R. and Nealson, K.H. (1990) J. Bacteriol. 172, 6232–6238.

[9] Pessanha, M., Brennan, L., Xavier, A.V., Cuthbertson, P.M., Reid, G.A., Chapman, S.K., Turner, D.L. and Salgueiro, C.A. (2001) FEBS Lett. 489, 8–13.

[10] Taylor, P., Pealing, S.L., Reid, G.A., Chapman, S.K. and Walkinshaw, M.D. (1999) Nat. Struct. Biol. 6, 1108–1112.

[11] Pealing, S.L., Black, A.C., Manson, F.D.C., Ward, F.B., Chapman, S.K. and Reid, G.A. (1992) Biochemistry 31, 12132–12140.

[12] Myers, C.R. and Myers, J.M. (1992) FEMS Microbiol. Lett. 98, 13–19.

[13] Leys, D., Meyer, T.E., Tsapin, A.S., Nealson, K.H., Cusanovich, M.A. and Van Beeumen, J.J. (2002) J. Biol. Chem. 277, 35703–35711.

[14] Turner, D.L. (1993) Eur. J. Biochem. 211, 563–568.

[15] Turner, D.L., Salgueiro, C.A., Schenkels, P., LeGall, J. and Xavier, A.V. (1995) Biochim. Biophys. Acta 1246, 24–28.

[16] Louro, R.O., Correia, I.J., Brennan, L., Coutinho, I.B., Turner, D.L. and Xavier, A.V. (1998) J. Am. Chem. Soc. 120, 13240–13247.

[17] Turner, D.L., Brennan, L., Messias, A.C., Teodoro, M.L. and Xavier, A.V. (2000) Eur. Biophys. J. 29, 104–112.

[18] Bertini, I., Luchinat, C., Parigi, G. and Walker, F.A. (1999) J. Biol. Inorg. Chem. 4, 515–519.

[19] Turner, D.L. (2000) J. Biol. Inorg. Chem. 5, 328–332.

[20] Quinn, R., Valentine, J.S., Byrn, M.P. and Strouse, C.E. (1987) J. Am. Chem. Soc. 109, 3301–3308.

[21] Barry, C.D., North, A.C., Glasel, J.A., Williams, R.J. and Xavier, A.V. (1971) Nature 232, 236–245.

[22] Banci, L., Bertini, I., Bren, K.L., Cremonini, M.A., Gray, H.B., Luchinat, C. and Turano, P. (1996) J. Biol. Inorg. Chem. 1, 117–126.

[23] Turner, D.L., Brennan, L., Chamberlin, S.G., Louro, R.O. and Xavier, A.V. (1998) Eur. Biophys. J. 27, 367–375.

[24] Banci, L., Bertini, I., Cavallaro, G. and Luchinat, C. (2002) J. Biol. Inorg. Chem. 7, 416–426.

[25] Pierattelli, R., Banci, L. and Turner, D.L. (1996) J. Biol. Inorg. Chem. 1, 320–329.

[26] Salgueiro, C.A., Turner, D.L., LeGall, J.L. and Xavier, A.V. (1997) J. Biol. Inorg. Chem. 2, 343–349.

[27] Turner, D.L. (1995) Eur. J. Biochem. 227, 829–837.

[28] Palmer, G. (2000) in: Physical Methods in Bioinorganic Chemistry (Que Jr., L., Ed.), pp. 121–186, University Science Books, Sausalito.

[29] Brennan, L. and Turner, D.L. (1997) Biochim. Biophys. Acta 1342, 1–12.

[30] Tsapin, A.I., Nealson, K.H., Meyers, T., Cusanovich, M.A., Van Beuumen, J., Crosby, L.D., Feinberg, B.A. and Zhang, C. (1996) J. Bacteriol. 178, 6386–6388.

[31] Brennan, L., Turner, D.L., Messias, A.C., Teodoro, M.L., LeGall, J., Santos, H. and Xavier, A.V. (2000) J. Mol. Biol. 298, 61–82.